$$E_{k\,\text{pos}}^{(e)} = \frac{1}{2}\int_0^l A\,(x)\boldsymbol{v}(x)^T\boldsymbol{v}(x)\rho dx,\ E_{k\,\text{sfer}}^{(e)} = \frac{1}{2}\int_0^l \boldsymbol{\omega}^T(x)\boldsymbol{J}(x)\boldsymbol{\omega}(x)\rho \mathrm{d}x, \quad (4)$$

where $A(x)$ is the cross-sectional area, ρ is the density of the material, and $\boldsymbol{J}(x) = diag\left(J_p(x), J(x), J(x)\right)$ is a diagonal matrix defined in terms of polar $J_p(x)$ and quadratic $J(x)$ moments of the shaft section. Substituting relations (1) - (2) into (4), we obtain:

$$E_{k\,\text{pos}}^{(e)} = \frac{1}{2}\int_0^l A\,(x)\big[\dot{u}^2\,(x) + \dot{v}^2\,(x) + \dot{w}^2\,(x) - 2\,\dot{v}\,(x)\omega_0 w(x) + 2\,\dot{w}\,(x)\omega_0 v(x) + \\ +\big(w^2(x) + v^2(x)\big)\omega_0^2\big]\rho \mathrm{d}x,$$

$$E_{k\,\text{sfer}}^{(e)} = \frac{1}{2}\int_0^l \Big[J_p(x)\left(\omega_0^2 + 2\omega_0\,\dot{\varphi}\,(x) + \dot{\varphi}^2\,(x)\right) + J(x)\left(\omega_0^2\psi^2(x) - 2\omega_0\psi(x)\,\dot{\vartheta}\,(x) + \\ + \dot{\vartheta}^2\,(x)\right) + J(x)\left(\omega_0^2\vartheta^2(x) + 2\omega_0\vartheta(x)\,\dot{\psi}\,(x) + \dot{\psi}^2\,(x)\right)\Big]\,\rho \mathrm{d}x. \quad (5)$$

The potential energy of the strained e-th finite element of the shaft is determined as:

$$E_p^{(e)} = \frac{1}{2}\int_0^l \int_{(A(x))} \left[E\varepsilon_x^2(x) + G\left(\gamma_{xy}^2(x) + \gamma_{xz}^2(x)\right)\right] dA(x)dx, \quad (6)$$

where E is the tensile modulus and G is the shear elastic modulus of the material.

Assuming the incompressibility of the cross-section of the shaft, we can determine the components of the displacement vector of an arbitrary point of the shaft relative to $\psi(x) = v'(x)$, $\vartheta(x) = -w'(x)$, i.e.:

$$\varepsilon_x = u'(x) - yv''(x) - zw''(x), \gamma_{xy} = -z\varphi'(x), \gamma_{xz} = y\varphi'(x). \quad (7)$$

Substitution of (7) into the expression for potential energy (6) results in:

$$E_p^{(e)} = \frac{1}{2}\int_0^l \int_{(A(x))} \left[E\big(u'(x) - yv''(x) - zw''(x)\big)^2 + G\varphi'^2(x)(y^2 + z^2)\right] \mathrm{d}A(x)\mathrm{d}x. \quad (8)$$

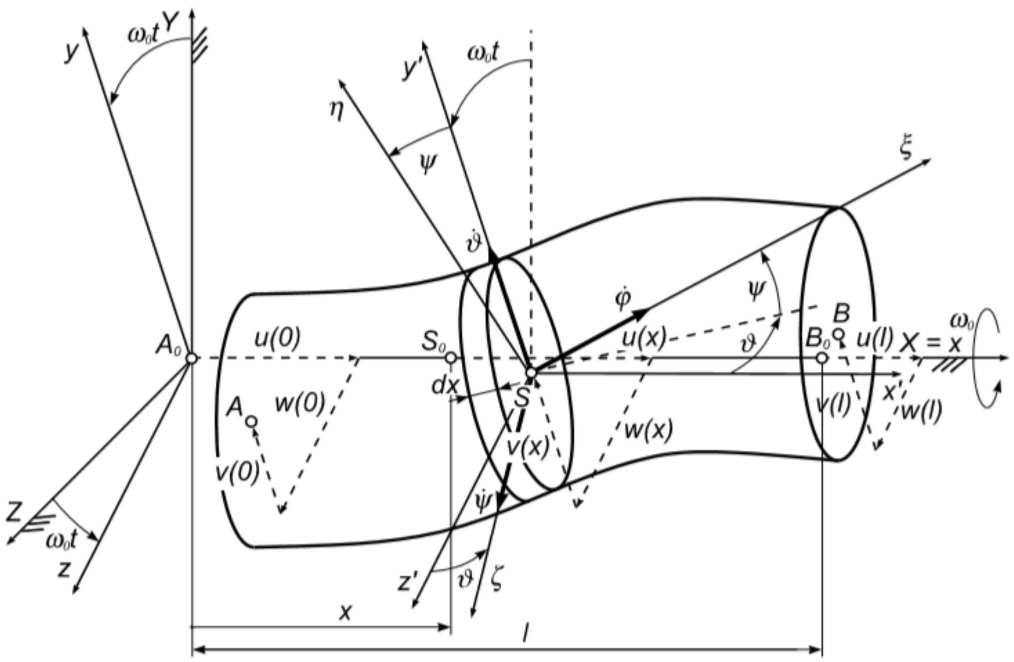

Fig.1. Scheme of the e-th finite element detailed from the circular section shaft

The components of the displacement vector inside the e-th finite element of the shaft are approximated by a linear and cubic function (a polynomial), i.e.:

$$v(x) = \boldsymbol{\Phi}(x)\boldsymbol{c}_1,\ \psi(x) = v'(x) = \boldsymbol{\Phi}'(x)\boldsymbol{c}_1, u(x) = \boldsymbol{\Psi}(x)\boldsymbol{c}_3,\ \varphi(x) = \boldsymbol{\Psi}(x)\boldsymbol{c}_4,$$
$$w(x) = \boldsymbol{\Phi}(x)\boldsymbol{c}_2,\ \vartheta(x) = -w'(x) = -\boldsymbol{\Phi}'(x)\boldsymbol{c}_2, \boldsymbol{\Phi}(x) = [1\ x\ x^2\ x^3], \boldsymbol{\Psi}(x) = [1\ x]. \quad (9)$$

To describe the strained state of the e-th finite element of the shaft in the xyz coordinate system, we use the vector of generalized displacements of the nodes A (for $x = 0$) and B (for $x = l$)

$$\tilde{\boldsymbol{q}}^{(e)} = [\boldsymbol{q}_1^T \boldsymbol{q}_2^T \boldsymbol{q}_3^T \boldsymbol{q}_4^T]^T, \tag{10}$$

where

$$\boldsymbol{q}_1 = \begin{bmatrix} v(0) \\ \psi(0) \\ v(x) \\ \psi(x) \end{bmatrix},\ \boldsymbol{q}_2 = \begin{bmatrix} w(0) \\ \vartheta(0) \\ w(x) \\ \vartheta(x) \end{bmatrix},\ \boldsymbol{q}_3 = \begin{bmatrix} u(0) \\ u(l) \end{bmatrix},\ \boldsymbol{q}_4 = \begin{bmatrix} \varphi(0) \\ \varphi(l) \end{bmatrix}. \tag{11}$$

Using approximation relations (9) for the end nodes A and B of the shaft, we obtain

$$\boldsymbol{q}_i = \boldsymbol{S}_i \boldsymbol{c}_i,\ i = 1,2,3,4, \tag{12}$$

where $$\boldsymbol{S}_1 = \begin{bmatrix} 1 & 0 & 0 & 0 \\ 0 & 1 & 0 & 0 \\ 1 & l & l^2 & l^3 \\ 0 & 1 & 2l & 3l^2 \end{bmatrix},\ \boldsymbol{S}_2 = \begin{bmatrix} 1 & 0 & 0 & 0 \\ 0 & -1 & 0 & 0 \\ 1 & l & l^2 & l^3 \\ 0 & -1 & -2l & -3l^2 \end{bmatrix},\ \boldsymbol{S}_3 = \begin{bmatrix} 1 & 0 \\ 1 & l \end{bmatrix}. \tag{13}$$

Eliminating the unknown vectors $\boldsymbol{c}_i$ of the coefficient of approximating functions (12), we obtain approximation relations connecting the components of the displacement and strain vector through the generalized displacements of the nodes, i.e.:

$$\boldsymbol{u}(x) = \boldsymbol{\Psi}(x)\boldsymbol{S}_3^{-1}\boldsymbol{q}_3, \boldsymbol{v}(x) = \boldsymbol{\Phi}(x)\boldsymbol{S}_1^{-1}\boldsymbol{q}_1, \boldsymbol{w}(x) = \boldsymbol{\Phi}(x)\boldsymbol{S}_2^{-1}\boldsymbol{q}_2,$$
$$\boldsymbol{\psi}(x) = \boldsymbol{\Phi}'(x)\boldsymbol{S}_1^{-1}\boldsymbol{q}_1, \boldsymbol{\vartheta}(x) = -\boldsymbol{\Phi}'(x)\boldsymbol{S}_2^{-1}\boldsymbol{q}_2, \boldsymbol{\varphi}(x) = \boldsymbol{\Psi}(x)\boldsymbol{S}_3^{-1}\boldsymbol{q}_4. \tag{14}$$

The kinetic (5) and potential energy (8) of the e-th finite element of the shaft can be rewritten in matrix form using the approximation relations (14)

$$E_k^{(e)} = \frac{1}{2}\left(\dot{\tilde{\boldsymbol{q}}}^{(e)}\right)^T \tilde{\boldsymbol{M}}^{(e)} \dot{\tilde{\boldsymbol{q}}}^{(e)} + \omega_0 \left(\dot{\tilde{\boldsymbol{q}}}^{(e)}\right)^T \tilde{\boldsymbol{C}}^{(e)} \tilde{\boldsymbol{q}}^{(e)} + \frac{1}{2}\omega_0^2 \left(\tilde{\boldsymbol{q}}^{(e)}\right)^T \tilde{\boldsymbol{K}}_d^{(e)} \tilde{\boldsymbol{q}}^{(e)} +$$
$$+\omega_0 \left(\dot{\tilde{\boldsymbol{q}}}^{(e)}\right)^T \tilde{\boldsymbol{f}}_1^{(e)} + \frac{1}{2}\omega_0^2 I^{(e)}, \quad E_p^{(e)} = \frac{1}{2}\left(\tilde{\boldsymbol{q}}^{(e)}\right)^T \tilde{\boldsymbol{K}}_s^{(e)} \tilde{\boldsymbol{q}}^{(e)}, \tag{15}$$

where $\tilde{\boldsymbol{M}}^{(e)}$ is the mass matrix, $\tilde{\boldsymbol{C}}^{(e)}$ is the Coriolis matrix, $\tilde{\boldsymbol{K}}_d^{(e)}$ is the reduced rotation matrix, $\tilde{\boldsymbol{f}}_1^{(e)}$ is the vector of gyroscopic forces, acting on the e-th finite element, $\tilde{\boldsymbol{K}}_s^{(e)}$ is the static stiffness matrix and $I^{(e)}$ is the moment of inertia of the e-th finite element of the shaft, which expresses the kinetic energy of a rotating unstrained element that rotates with a constant angular velocity ω_0.

The matrix and vector of the e-th finite element of the shaft have the following form:

$$\tilde{\boldsymbol{M}}^{(e)} = \begin{bmatrix} \boldsymbol{S}_1^{-T}(\boldsymbol{I}_1 + \boldsymbol{I}_2)\boldsymbol{S}_1^{-1} & \boldsymbol{0} & \boldsymbol{0} & \boldsymbol{0} \\ \boldsymbol{0} & \boldsymbol{S}_2^{-T}(\boldsymbol{I}_1 + \boldsymbol{I}_2)\boldsymbol{S}_2^{-1} & \boldsymbol{0} & \boldsymbol{0} \\ \boldsymbol{0} & \boldsymbol{0} & \boldsymbol{S}_3^{-T}\boldsymbol{I}_4\boldsymbol{S}_3^{-1} & \boldsymbol{0} \\ \boldsymbol{0} & \boldsymbol{0} & \boldsymbol{0} & \boldsymbol{S}_3^{-T}\boldsymbol{I}_5\boldsymbol{S}_3^{-1} \end{bmatrix}, \tag{16}$$

$$\tilde{\boldsymbol{C}}^{(e)} = \begin{bmatrix} \boldsymbol{0} & -\boldsymbol{S}_1^{-T}(\boldsymbol{I}_1 + \boldsymbol{I}_2)\boldsymbol{S}_2^{-1} & \boldsymbol{0} & \boldsymbol{0} \\ \boldsymbol{S}_2^{-T}(\boldsymbol{I}_1 + \boldsymbol{I}_2)\boldsymbol{S}_1^{-1} & \boldsymbol{0} & \boldsymbol{0} & \boldsymbol{0} \\ \boldsymbol{0} & \boldsymbol{0} & \boldsymbol{0} & \boldsymbol{0} \\ \boldsymbol{0} & \boldsymbol{0} & \boldsymbol{0} & \boldsymbol{0} \end{bmatrix}, \tag{17}$$

$$\tilde{\boldsymbol{K}}_d^{(e)} = \begin{bmatrix} \boldsymbol{S}_1^{-T}(\boldsymbol{I}_1 + \boldsymbol{I}_2)\boldsymbol{S}_2^{-1} & \boldsymbol{0} & \boldsymbol{0} & \boldsymbol{0} \\ \boldsymbol{0} & \boldsymbol{S}_2^{-T}(\boldsymbol{I}_1 + \boldsymbol{I}_2)\boldsymbol{S}_2^{-1} & \boldsymbol{0} & \boldsymbol{0} \\ \boldsymbol{0} & \boldsymbol{0} & \boldsymbol{0} & \boldsymbol{0} \\ \boldsymbol{0} & \boldsymbol{0} & \boldsymbol{0} & \boldsymbol{0} \end{bmatrix}, \tag{18}$$

$$\tilde{\boldsymbol{K}}_s^{(e)} = \begin{bmatrix} \boldsymbol{S}_1^{-T}\boldsymbol{I}_3\boldsymbol{S}_1^{-1} & \boldsymbol{0} & \boldsymbol{0} & \boldsymbol{0} \\ \boldsymbol{0} & \boldsymbol{S}_2^{-T}\boldsymbol{I}_3\boldsymbol{S}_2^{-1} & \boldsymbol{0} & \boldsymbol{0} \\ \boldsymbol{0} & \boldsymbol{0} & \boldsymbol{S}_3^{-T}\boldsymbol{I}_6\boldsymbol{S}_3^{-1} & \boldsymbol{0} \\ \boldsymbol{0} & \boldsymbol{0} & \boldsymbol{0} & \boldsymbol{S}_3^{-T}\boldsymbol{I}_7\boldsymbol{S}_3^{-1} \end{bmatrix}, \tag{19}$$

$$\tilde{\boldsymbol{f}}_1^{(e)} = [\boldsymbol{0} \quad \boldsymbol{0} \quad \boldsymbol{0}\ \boldsymbol{I}_8^T\boldsymbol{S}_3^{-1}]^T. \tag{20}$$

Here the quantities in (16) - (20) have the form:

$$\boldsymbol{I}_1 = \int_0^l \rho A(x)\,\boldsymbol{\Phi}^T(x)\boldsymbol{\Phi}(x)dx, \qquad \boldsymbol{I}_2 = \int_0^l \rho J(x)\,\boldsymbol{\Phi}'^T(x)\boldsymbol{\Phi}'(x)dx,$$

$$\boldsymbol{I}_3 = \int_0^l EJ(x)\,\boldsymbol{\Phi}''^T(x)\boldsymbol{\Phi}''(x)dx, \qquad \boldsymbol{I}_4 = \int_0^l \rho A(x)\,\boldsymbol{\Psi}^T(x)\boldsymbol{\Psi}(x)dx,$$

$$\boldsymbol{I}_5 = 2\int_0^l \rho J(x)\,\boldsymbol{\Psi}^T(x)\boldsymbol{\Psi}(x)dx, \qquad \boldsymbol{I}_6 = \int_0^l EA(x)\,\boldsymbol{\Psi}'^T(x)\boldsymbol{\Psi}'(x)dx,$$

$$\boldsymbol{I}_7 = 2\int_0^l GJ(x)\,\boldsymbol{\Psi}'^T(x)\boldsymbol{\Psi}'(x)dx, \qquad \boldsymbol{I}_8 = 2\int_0^l \rho J(x)\,\boldsymbol{\Psi}^T(x)dx\,. \tag{21}$$

The values that include the spherical motion of the shaft are represented by integral matrices $\boldsymbol{I}_2$ and $\boldsymbol{I}_5$.

In the case of a prismatic shaft ($A\,(x) = A,\ J(x) = J$), the integral matrices in (21) have the form

$$\boldsymbol{I}_1 = \varrho A l \begin{bmatrix} 1 & l/2 & l^2/3 & l^3/4 \\ l/2 & l^2/3 & l^3/4 & l^4/5 \\ l^2/3 & l^3/4 & l^4/5 & l^5/6 \\ l^3/4 & l^4/5 & l^5/6 & l^6/7 \end{bmatrix}, \qquad \boldsymbol{I}_2 = \varrho J l \begin{bmatrix} 0 & 0 & 0 & 0 \\ 0 & 1 & l & l^2 \\ 0 & l & 4l^2/3 & 3l^3/2 \\ 0 & l^2 & 3l^3/2 & 9l^4/5 \end{bmatrix}$$

$$\boldsymbol{I}_3 = EJl \begin{bmatrix} 0 & 0 & 0 & 0 \\ 0 & 0 & 0 & 0 \\ 0 & 0 & 4 & 6l \\ 0 & 0 & 6l & 12l^2 \end{bmatrix}, \ \boldsymbol{I}_4 = \varrho A l \begin{bmatrix} 1 & l/2 \\ l/2 & l^2/3 \end{bmatrix}, \ \boldsymbol{I}_5 = \varrho J_p l \begin{bmatrix} 1 & l/2 \\ l/2 & l^2/3 \end{bmatrix},$$

$$\boldsymbol{I}_6 = EAl \begin{bmatrix} 0 & 0 \\ 0 & 1 \end{bmatrix}, \ \boldsymbol{I}_7 = GJ_p l \begin{bmatrix} 0 & 0 \\ 0 & 1 \end{bmatrix}, \tag{22}$$

where $J_p = 2J$, ϱ is the density of the material, E and G are the constants of the elastic material (i.e., the moduli of elasticity under tension and shear).

After discretizing the one-dimensional continuum (a shaft) into finite elements and using the finite element method procedure and (15), with corresponding matrices, vectors for finite elements and the permutation matrix $\boldsymbol{P}\epsilon\boldsymbol{R}^{12,12}$ $\boldsymbol{X}^{(e)} = \boldsymbol{P}^T\widetilde{\boldsymbol{X}}^{(e)}\boldsymbol{P}$, $\boldsymbol{X} = \boldsymbol{M}, \boldsymbol{C}, \boldsymbol{K}_d, \boldsymbol{K}_s$, we obtain the following expression for the energy for the shaft (a continuum)

$$E_k = \sum_{e=1}^{N} E_k^{(e)} = \frac{1}{2}\boldsymbol{q}^T\boldsymbol{M}\dot{\boldsymbol{q}} + \omega_0(\dot{\boldsymbol{q}})^T\boldsymbol{C}\boldsymbol{q} + \frac{1}{2}\omega_0^2(\boldsymbol{q})^T\boldsymbol{K}_d\boldsymbol{q} + \omega_0(\dot{\boldsymbol{q}})^T\boldsymbol{f}_1 + \frac{1}{2}\omega_0^2 I,$$

$$E_p = \sum_{e=1}^{N} E_p^{(e)} = \frac{1}{2}(\boldsymbol{q})^T\boldsymbol{K}_s\boldsymbol{q}, \tag{23}$$

where N is the number of finite elements into which the considered shaft is partitioned, $\boldsymbol{M}$ is the global mass matrix, $\boldsymbol{C}$ is the global Coriolis matrix, $\boldsymbol{f}_1$ is the global vector of gyroscopic forces, $\boldsymbol{I}$ is the total moment of inertia of the shaft around the $\boldsymbol{x}$ axis, $\boldsymbol{K}_d$ is the global matrix of rotating reduction, $\boldsymbol{K}_s$ is the global static stiffness matrix, and $\boldsymbol{q}$ is the matrix of the global vector of node deviations (generalized coordinate vector), in the form

$$\boldsymbol{q} = [\boldsymbol{q}_i],\ \boldsymbol{q}_i = [u(x), v(x), w(x), \varphi(x), \vartheta(x), \psi(x)]^T,\ i = 1,2,\dots,N,N+1. \tag{24}$$

The Lagrange equations for the shaft (without damping and external excitation) in matrix form can be written as

$$\frac{d}{dt}\left(\frac{\partial E_k}{\partial \dot{\boldsymbol{q}}}\right) - \left(\frac{\partial E_k}{\partial \boldsymbol{q}}\right) + \left(\frac{\partial E_p}{\partial \boldsymbol{q}}\right) = 0. \tag{25}$$

Substituting the expression for the kinetic and potential energy (23) into the Lagrange equations (25), we obtain a system of ordinary differential equations in matrix form describing the motion of a rotating shaft taking into account the above factors, i.e.:

$$\boldsymbol{M}\ddot{\boldsymbol{q}}(t) + \omega_0 \boldsymbol{G}\dot{\boldsymbol{q}}(t) + (\boldsymbol{K}_s - \omega_0^2 \boldsymbol{K}_d)\boldsymbol{q}(t) = \boldsymbol{0}. \tag{26}$$

Here: $\omega_0 \boldsymbol{G} = \omega_0(\boldsymbol{C} - \boldsymbol{C}^T)$ is the global matrix of gyroscopic effects.

Simulation of dynamic processes in the rigid disks. The rigid disk model can be used as a simplified model of gears, couplings, wheels of railway vehicles, etc.

Therefore, in this section, we will consider the constructed mathematical model for describing dynamic processes in the rigid disks in rotating coordinates. For this, a disk (Fig. 2) is considered with mass m as a rotating symmetric one and it has a center of mass at point S. Suppose that the origin of the Cartesian coordinate system $\xi\eta\zeta$ is at the center of mass of the disk, i.e. at point S and the coordinate system is rigidly connected to the disk. Then the distribution of the disk weight can be described by the inertia matrix $I_S = diag(I_0,\ I,\ I)$, in which these moments of inertia were determined around individual axes $I_0 = I_\xi,\ I = I_\eta = I_\zeta$ [4]. Further, considering the second Cartesian coordinate system xyz, which rotates around the x-axis with a constant angular velocity ω_0, which corresponds to the nominal angular velocity of the body ω. The oscillatory motion of the disk is described by displacements u, v, and w, respectively, in the directions of the x, y, and z axes and at the Euler angles of φ, ϑ, and ψ. The general spatial motion of the body is resolved into translational motion, described by a velocity vector with components in a rotating coordinate xyz as

$$\boldsymbol{v_S}\,(\boldsymbol{t}) = \begin{bmatrix} \dot{\boldsymbol{u}}(\boldsymbol{t}) \\ \dot{\boldsymbol{v}}(\boldsymbol{t}) - \boldsymbol{\omega_0 w}(\boldsymbol{t}) \\ \dot{\boldsymbol{w}}(\boldsymbol{t}) + \boldsymbol{\omega_0 v}(\boldsymbol{t}) \end{bmatrix}, \tag{27}$$

and the relative spherical motion around the center of mass of the disk S, which is determined in the coordinate system $\xi\eta\zeta$ by the angular velocity vector

$$\boldsymbol{\omega}(\boldsymbol{t}) = \begin{bmatrix} \boldsymbol{\omega_0}\, \boldsymbol{cos}(\boldsymbol{\vartheta}(\boldsymbol{t}))\, \boldsymbol{cos}(\boldsymbol{\psi}(\boldsymbol{t})) + \dot{\boldsymbol{\vartheta}}(\boldsymbol{t})\, \boldsymbol{sin}(\boldsymbol{\psi}(\boldsymbol{t})) + \dot{\boldsymbol{\varphi}}(\boldsymbol{t}) \\ \dot{\boldsymbol{\vartheta}}(\boldsymbol{t})\, \boldsymbol{cos}(\boldsymbol{\psi}(\boldsymbol{t})) - \boldsymbol{\omega_0}\, \boldsymbol{cos}(\boldsymbol{\vartheta}(\boldsymbol{t}))\boldsymbol{sin}(\boldsymbol{\psi}(\boldsymbol{t})) \\ \dot{\boldsymbol{\psi}}(\boldsymbol{t}) + \boldsymbol{\omega_0 sin}(\boldsymbol{\vartheta}(\boldsymbol{t})) \end{bmatrix}. \tag{28}$$

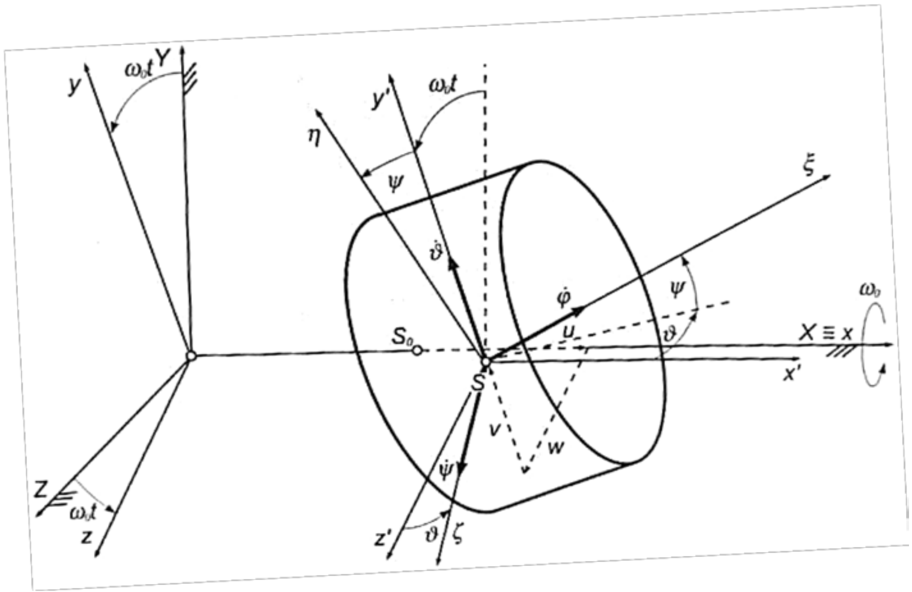

Fig. 2. Rigid disk in a rotating coordinate system

Taking into account the smallness of the angles of rotation ($\dot{\varphi}, \dot{\vartheta} \ll \omega_0$), expression (28) can be simplified, i.e.:

$$\boldsymbol{\omega}(\mathbf{t}) = \begin{bmatrix} \boldsymbol{\omega_0} + \dot{\boldsymbol{\vartheta}}(\mathbf{t})\boldsymbol{\psi}(\mathbf{t}) + \dot{\boldsymbol{\varphi}}(\mathbf{t}) \\ \dot{\boldsymbol{\vartheta}}(\mathbf{t}) - \boldsymbol{\omega_0}\boldsymbol{\psi}(\mathbf{t}) \\ \dot{\boldsymbol{\psi}}(\mathbf{t}) + \boldsymbol{\omega_0}\boldsymbol{\vartheta}(\mathbf{t}) \end{bmatrix}. \tag{29}$$

In this case, the kinetic energy of the disk is determined as follows:

$$E_k = \frac{1}{2} m\boldsymbol{v}_S^T\boldsymbol{v}_S + \frac{1}{2} \boldsymbol{\omega}^T \boldsymbol{I}_S\boldsymbol{\omega}. \tag{30}$$

After substituting (27) and (29) into (30) and after some correction, we get:

$$E_k = \frac{1}{2}m\dot{u}^2 + \frac{1}{2}m(\dot{v} - \omega_0 w)^2 + \frac{1}{2}m(\dot{w} + \omega_0 v)^2 + \frac{1}{2}[I_0 (\omega_0 + \dot{\varphi})^2 + 2\omega_0\dot{\vartheta}\psi] + \\ + \frac{1}{2}I\left(\dot{\vartheta} - \omega_0\psi\right)^2 + \frac{1}{2}I(\dot{\psi} + \omega_0\vartheta)^2 . \tag{31}$$

Substituting (31) into the Lagrange equation allows us to obtain a system of ordinary differential equations in matrix form which describes the motion of a rigid disk:

$$\frac{d}{dt}\left(\frac{\partial E_k}{\partial \dot{\boldsymbol{q}}_D}\right) - \left(\frac{\partial E_k}{\partial \boldsymbol{q}_D}\right) + \left(\frac{\partial E_p}{\partial \boldsymbol{q}}\right) = \boldsymbol{M}_D\ddot{\boldsymbol{q}}_D(t) + \omega_0\boldsymbol{G}_D\dot{\boldsymbol{q}}_D(t) + (\omega_0^2\boldsymbol{K}_D)\boldsymbol{q}_D(t). \tag{32}$$

Here: $\boldsymbol{q}_D(t) = [u, v, w, \varphi, \vartheta, \psi]^T$ is the vector of generalized coordinates of the rigid disk. At that, $\boldsymbol{M}_D$ are the rigid disk mass matrices, which have the form:

$$\boldsymbol{M}_D = diag\,(m, m, m, I_0, I, I), \tag{33}$$

and the gyroscopic effect matrices of the rigid disk are:

$$\boldsymbol{G}_D = \begin{bmatrix} 0 & 0 & 0 & 0 & 0 & 0 \\ 0 & 0 & -2m & 0 & 0 & 0 \\ 0 & 2m & 0 & 0 & 0 & 0 \\ 0 & 0 & 0 & 0 & 0 & 0 \\ 0 & 0 & 0 & 0 & 0 & I_0 - 2I \\ 0 & 0 & 0 & 0 & 2I - I_0 & 0 \end{bmatrix}. \tag{34}$$

The rigid disk reduced rotation matrix $\boldsymbol{K}_{D\omega}$ is diagonal and has the form:

$$\boldsymbol{K}_{D\omega} = diag(0, m, m, 0, I, I). \tag{35}$$

It should be noted that for axisymmetric bodies in the form of a thin disk, $I_0 = 2I$ holds; it means the relationship between I_0 – the moment of inertia about the axis of rotation and I – the moment of inertia of the cross-section of the disk. More information on modeling rigid and flexible disks in dynamic processes is described in detail in the monograph [4].

3. Results and discussion

In this study, the determination of the dynamic characteristics (i.e., eigenfrequencies, modes, and decrement of oscillations) of a specific system (an object) is performed using the Altair Hyperworks and MATLAB software packages.

The dynamic characteristics of the system are determined by solving the problem of natural vibrations for the system under consideration. Natural vibrations are the most ordered motions of the system, occurring in the absence of external influences; all points of the system oscillate according to the same real or complex harmonic law, with different amplitudes. In this case, the real part of the complex eigenfrequency means the frequency of oscillations of the system, and the imaginary part determines the velocity of oscillation damping and has the meaning of the damping coefficient.

Determining the dynamic characteristics of a system is an important part of any dynamic analysis and it allows evaluating the dynamic behavior of a system (an object). When studying the natural vibrations of the system (determining the dynamic characteristics), a homogeneous system of ordinary differential equations (26) or (32) is solved.

The described method was used to evaluate the eigenfrequencies and modes of vibration of a simple test steel shaft of wheelsets mounted on two bearings (radial-axial and radial ones).

The tested wheelsets consist of a hollow shaft and two disks (Fig. 3). Calculations were made for wheelsets with the following parameters - geometric dimensions: inner diameter of the shaft d_{shaft} = 0.026 m; outer diameters of the shaft $D_1 = 0{,}130\ m$, $D_2 = 0{,}165\ m$, $D_3 = 0.194\ m, D_4 = 0.1475$ m, $D_5 = 0.179\ m$; the length of the shaft l = 2.216 m; bearing stiffness $k_b = 6e + 12\ [N/m]$, $k_a = 2e + 12\ [N/m]$; the moment of inertia of the disks $I_{10} = I_{20} = 54.69\ kg \cdot m^2, I_1 = I_2 = 27.88\ kg \cdot m^2$; mass of disks $m_1 = m_2 = 364.57$ kg; material properties: modulus of elasticity E = 2.1e+11 Pa, G = 8.076e+10 Pa; Poisson's ratio ν = 0.30; specific gravity of the material ρ = 7850 kg/m^3.

Determination of the dynamic characteristics of a rotating wheelset without damping. In the case of non-rotating wheelsets (for $\omega_0 = 0$ rad/s), taking into account the bearings, the system of equations of motion has the following form:

$$\left(\boldsymbol{M} + \boldsymbol{M}_1^{(D)} + \boldsymbol{M}_2^{(D)}\right)\ddot{\boldsymbol{q}}(t) + (\boldsymbol{K_s} + \boldsymbol{K_B})\boldsymbol{q}(t) = \boldsymbol{0}, \tag{36}$$

where $\boldsymbol{K_B}$ - is the bearing stiffness matrix, $\boldsymbol{M}_1^{(D)}, \boldsymbol{M}_2^{(D)}$ are the disk mass matrices.

The system of equations (36) for determining the generalized eigenvalue problem can be written in the form

$$\left[(\boldsymbol{K_s} + \boldsymbol{K_B}) - \lambda_\nu\left(\boldsymbol{M} + \boldsymbol{M}_1^{(D)} + \boldsymbol{M}_2^{(D)}\right)\right]\boldsymbol{q} = \boldsymbol{0}, \tag{37}$$

where λ_ν – the roots of the characteristic equation are the eigenvalues equal to the square of the eigenfrequencies Ω_ν^2.

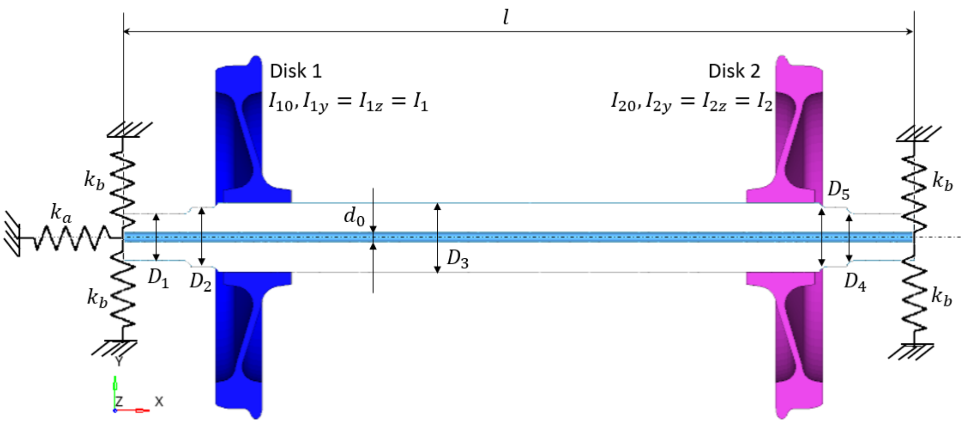

Fig. 3: Scheme of the tested wheelset

Table 1 shows the first eight eigenfrequencies $f_\nu = \Omega_\nu/2\pi$ of a non-rotating wheelset (as a deformable body) obtained using the Altair OptiStruct and MATLAB computer programs with short characteristics of the natural modes of vibration.

Table 1. Natural frequencies of the non-rotating wheelset

Number of eigenfrequencies f_ν	Eigenfrequency f_ν [Hz], MATLAB	Eigenfrequency f_ν [Hz], Altair OptiStruct	Mode of vibration	Error [%]
1	0	0	Uniform rotation of the entire system (without twisting the shaft)	0
2.3	57.83	57.64	Bending mode of vibrations	0.34
4	80.07	86.26	Torsional mode of vibrations	7.17
5.6	163.6	170.11	Bending mode of vibrations	3.84
7.8	354.11	363.08	Bending mode of vibrations	2.46

Figure 4 shows some natural modes of vibration of wheelsets corresponding to multiple eigenfrequencies.

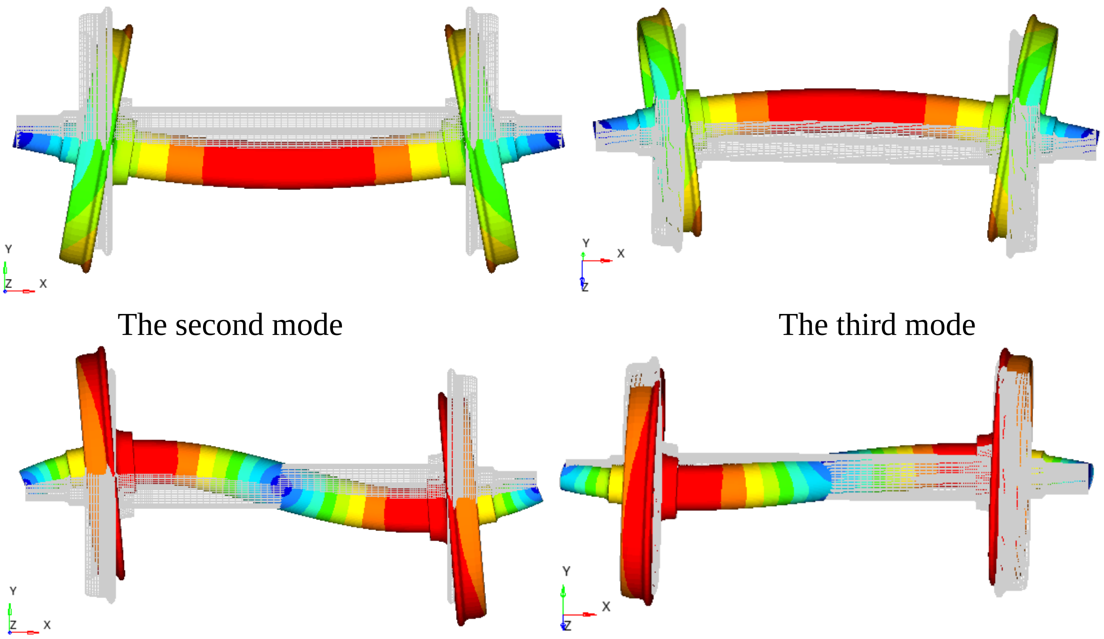

The second mode The third mode

The fifth mode The sixth mode

Fig. 4. Multiple natural modes of vibration of the non-rotating wheelset

Analysis of eigenfrequencies (Table 1) and modes of vibration (Fig. 4) shows that the first mode of vibration of rotating wheelsets is the motion of an absolutely rigid body with frequency $f_0 = 0$. An account for the elastic properties of the material of rotating shaft (as a deformable body) with two identical rigid disks leads to the appearance of multiple eigenfrequencies $f_{2,3}$ and $f_{5,6}$ with the corresponding modes of vibration.

In the case of a rotating shaft (at $\omega_0 \neq 0$ rad/s), the following aspects are taken into account: gyroscopic effects $(\omega_0(\boldsymbol{G}+\boldsymbol{G}_D)$ and the effect of rotation on the overall stiffness $(\omega_0^2(\boldsymbol{K}_d+\boldsymbol{K}_{D\omega})$.

The equation for determining the eigenvalues has the following form:

$$(\boldsymbol{K_s}+\boldsymbol{K_B}-\omega_0^2(\boldsymbol{K}_d+\boldsymbol{K}_{D\omega})\dot{\boldsymbol{q}}(t)-(\boldsymbol{K_s}+\boldsymbol{K_B}-\omega_0^2(\boldsymbol{K}_d+\boldsymbol{K}_{D\omega})\dot{\boldsymbol{q}}(t)=\boldsymbol{0}. \tag{38}$$

We transform the equation of motion (26) and (32) from the generalized coordinate space to the space $\boldsymbol{u}(\boldsymbol{t})=[\dot{\boldsymbol{q}}^{\boldsymbol{T}}(\boldsymbol{t}) \quad \boldsymbol{q}^{\boldsymbol{T}}(\boldsymbol{t})]^T$ of the state, that is, $\boldsymbol{u}(\boldsymbol{t}) \in \boldsymbol{R}^{\boldsymbol{2n}}$

$$\boldsymbol{S}\dot{\boldsymbol{u}}(t)+\boldsymbol{A}\boldsymbol{u}(\boldsymbol{t})=\boldsymbol{0}. \tag{39}$$

Here:

$$\boldsymbol{S}=\begin{bmatrix} (\boldsymbol{M}+\boldsymbol{M}_1^{(D)}+\boldsymbol{M}_2^{(D)}) & \boldsymbol{0} \\ \boldsymbol{0} & (\boldsymbol{K_s}+\boldsymbol{K_B}-\omega_0^2(\boldsymbol{K}_d+\boldsymbol{K}_{D\omega})\end{bmatrix} \text{ is an asymmetric matrix,} \tag{40}$$

$$\boldsymbol{A}=\begin{bmatrix} \omega_0(\boldsymbol{G}+\boldsymbol{G}_D) & (\boldsymbol{K_s}+\boldsymbol{K_B}-\omega_0^2(\boldsymbol{K}_d+\boldsymbol{K}_{D\omega}) \\ -(\boldsymbol{K_s}+\boldsymbol{K_B}-\omega_0^2(\boldsymbol{K}_d+\boldsymbol{K}_{D\omega}) & \boldsymbol{0}\end{bmatrix} \text{ is an antisymmetric matrix.} \tag{41}$$

With (39) - (41) the eigenvalue problem is written in the form of a system of a homogeneous algebraic equation:

$$[\boldsymbol{A}-\lambda_\nu \boldsymbol{S}]\boldsymbol{u}=\boldsymbol{0}. \tag{42}$$

A nontrivial solution to system (42) is λ_ν, that is, the eigenvalues of the characteristic determinant of equations (42), which are the imaginary value obtained due to the antisymmetry of the matrix $\omega_0(\boldsymbol{G}+\boldsymbol{G}_D)$.

The eigenvalues λ_ν of system (42) are a complex quantity, i.e. $\lambda_\nu = \pm i\Omega_\nu$, $\nu = 1, 2, \ldots, n$ and their imaginary part is the eigenfrequencies Ω_ν in rad/s of rotating wheelsets.

Figure 5 shows (full line) the dependence of the first eight eigenfrequencies $f_\nu = 2\pi\Omega_\nu$ (Hz) on the rotating speed of the wheelsets per minute (the so-called Campbell diagram) plotted in the angular velocity range from $\omega_0 = 0$ to $\omega_0 = 3500$ rpm.

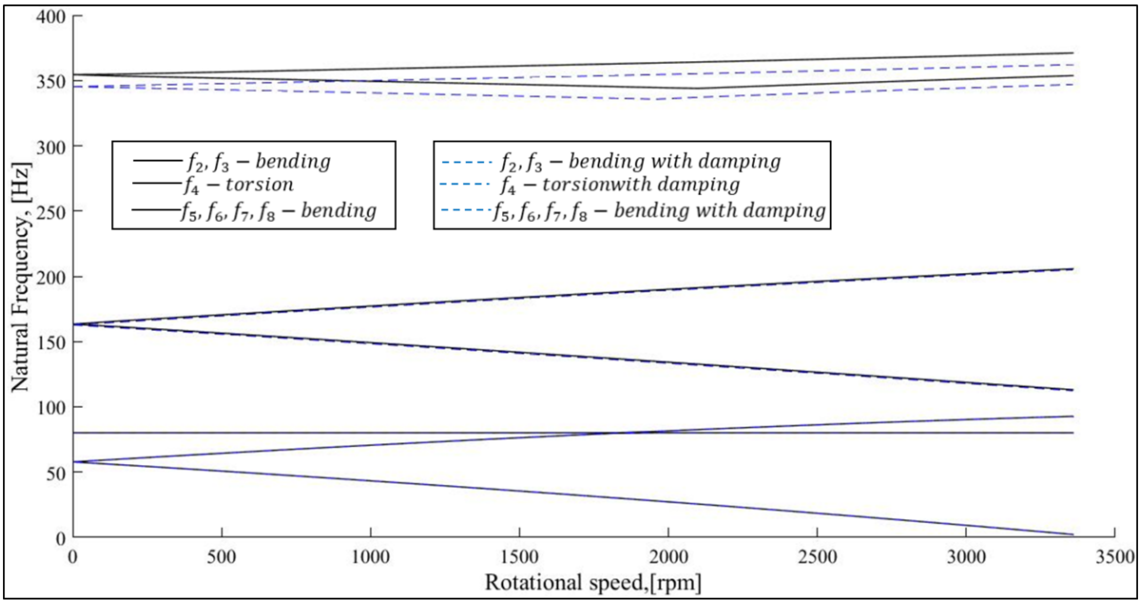

Fig. 5. Campbell diagram for rotating wheelset

Paired eigenfrequencies are divided into two branches, where the first increases and the second decreases depending on the angular velocity. This phenomenon is caused by gyroscopic effects. Obviously, the non-paired eigenfrequencies (f_4) do not depend on the rotating speed since this mode of vibrations does not affect the gyroscopic effects (torsional mode of vibrations).

Determination of dynamic characteristics of a rotating wheelset with damping. Rotating wheelsets are considered with an account for the damping properties of the shaft material. Generally, in the calculations, when solving practical problems in engineering, the damping matrix [12] is used, instead of viscous damping, in the form of a linear combination of the mass and stiffness matrices $\boldsymbol{B}_s = a\boldsymbol{M}_s + b\boldsymbol{K}_s$, a is the mass proportionality coefficient and b is the stiffness proportionality coefficient. The use of the damping matrix $\boldsymbol{B}_s = a\boldsymbol{M}_s + b\boldsymbol{K}_s$ simplifies the solution of practical problems.

When describing dynamic processes on a rotating shaft with rigid disks (wheelsets), with the damping coefficient, equation (42) $(\omega_0(\boldsymbol{G} + \boldsymbol{G}_D)$ is written using the damping matrix($\boldsymbol{B}_s$), in the form $(\omega_0(\boldsymbol{G} + \boldsymbol{G}_D) + \boldsymbol{B}_s)$.

Specific calculations for the geometrical and physical-mechanical parameters of the rotating shaft and rigid disk (wheelsets) similar to the given above were obtained. The relative damping coefficients were determined from [12] using α_ν and β_ν, for $\omega_0 = 700$ rad/s and $a = 0, b = 0.0002$.

Further, using the developed model, the eigenfrequencies and the damping coefficient for rotating wheelsets were determined, taking into account the damping properties of the shaft material (Table 2). The damping coefficient D_ν was determined by the formula

$$D_\nu = \frac{-\alpha_\nu}{\sqrt{\alpha_\nu^2 + \beta_\nu^2}}. \quad (43)$$

Eigenfrequencies of the rotating wheelsets, considering damping, are given in Table 2.

Table 2. Natural frequencies of rotating wheelsets

Number of eigenfrequencies ν	Eigenfrequency f_ν (Hz), not considering damping (for $\omega_0 = 700$ rad/s)	Damping coefficients D_ν,	Eigenfrequency f_ν(Hz), considering damping (for $\omega_0 = 700$ rad/s) $\lambda_\nu = \alpha_\nu \pm i\,\beta_\nu$	Damping coefficients D_ν,
1	$-3.84e-6 \pm i\,0$	1	$0,0027 \pm i\,0$	1
2	$-1.72e-5 \pm i47.88$	3.59e-07	$-1.75 \pm i47.84$	0.0366
3	$-1.06e-05 \pm i66.97$	1.58e-07	$-2.45 \pm i66.93$	0.0366
4	$-2.02e-07 \pm i80.11$	2.52e-09	$-4.03 \pm i79.97$	0.0503
5	$-1.2e-03 \pm i153.60$	7.84e-06	$-15.80 \pm i152.73$	0.1029
6	$-1.6e-03 \pm i173.24$	9.28E-06	$-17.83 \pm i172.36$	0.1029
7	$-5.21e-05 \pm i350.8$	1.49e-07	$-78.06 \pm i341.96$	0.2225
8	$-5.27e-05 \pm i357.4$	1.48e-07	$-79.54 \pm i348.51$	0.2225

Table 2 shows the first eight eigenfrequencies of a rotating shaft (as a deformable body) with wheelsets (at ω_0 = 700 rad/s) with and without damping, obtained using the MATLAB software. The results obtained show that an account for the damping affects only the seventh and eighth eigenfrequencies. Figure 5 shows (dashed line) the dependence of the first eight eigenfrequencies on the damping. The remaining (the first six) eigenfrequencies are practically not affected by damping.

4. Conclusions

1. Mathematical models and methods for determining the dynamic characteristics (eigenfrequencies, modes, and decrement of oscillations) of railway wheelsets, taking into account internal damping and gyroscopic effect were developed in this study.
2. The eigenfrequencies, modes, and damping coefficient of rotating wheelsets at their different revolutions with and without damping were investigated.
3. As a result of studying the dynamic characteristics of rotating wheelsets, it was determined that:

– the values of the paired eigenfrequencies (f_2, f_3, f_5, f_6 and f_7, f_8) were divided into two groups; in the first group the values of (f_2, f_5, and f_7) increased, and in the second group the values of (f_3, f_6 and f_8) decreased depending on the angular velocity due to the influence of the gyroscopic effect;

– non-multiple eigenfrequencies (i.e.,$-$ f_4) did not depend on the rotation velocity since the gyroscopic effects did not affect the torsional modes;

– the damping effect did not affect the first 5 eigenfrequencies (f_2, f_3, f_4, f_5 and f_6), and when damping was taken into account, the seventh and eighth frequencies f_7, f_8 decreased insignificantly.

References

[1] Krämer E. *Dynamics of Rotors and Foundations*. Berlin: Springer; 2012.
[2] Wittenburg J. *Dynamics of Multibody Systems*. 2nd ed. Wittenburg; 2008.
[3] Yamamoto T. *Linear and Nonlinear Rotordynamics: A Modern Treatment with Applications*. New York: Wiley Interscience; 2012.
[4] Eliseev V. *Mechanics of a deformable rigid body*. Publishing House of the Polytechnic University; 2006.
[5] Kaiyun W, Chao H, Wanming Z, Pengfei L, Shen W. Progress on wheel-rail dynamic performance of railway curve negotiation. *Journal of Traffic and Transportation Engineering*. 2014;1(3): 209-220.

[6] Trimpe F, Lück S, Naumann R, Salander C. Simulation of Torsional Vibration of Driven Railway Wheelsets Respecting the Drive Control Response on the Vibration Excitation in the Wheel-Rail Contact. *Vibration*. 2021;4(1): 30-48.

[7] Xiaoqi M, Lin J, Liangliang H. A computational simulation study on the dynamic response of high-speed wheel–rail system in rolling contact. *Advances in Mechanical Engineering*. 2018;10(11): 1-11.

[8] Mikheev G, Pogorelov D, Rodkov A. Methods of Simulation of Railway Wheelset Dynamics taking into account Elasticity. In: *Proc. First International Conference on Rail Transportation*. China; 2017. DOI: 10.13140/RG.2.2.32562.25281.

[9] Vila P, Rovira A, Fayos J, Baeza L. Dynamic model of a railway wheelset for corrugation problem analysis. *Journal Noise and Vibration Worldwide*. 2009;40(11): 10-17.

[10] Torstensson PT, Nielsen JCO, Baeza L. Dynamic train-track interaction at high vehicle speeds-Modelling of wheelset dynamics and wheel rotation. *Journal of Sound and Vibration*. 2011;330(22): 5309-5321.

[11] Uyulan C, Gokasan M, Bogosyan S. Dynamic Investigation of the Hunting Motion of a Railway Bogie in a Curved Track via Bifurcation Analysis. *Mathematical Problems in Engineering*. 2017: 8276245.

[12] Byrtus M, Hajžman M, Zeman V. *Dynamika rotujících soustav*. ZČU v Plzni; 2010. (In Czech)

[13] Bykov V, Melnikov A. Mathematical model of a flexible rotor based on generalized Lagrangian coordinates. *Bulletin of St. Petersburg University*. 2010;4: 110-118.

[14] Tian Y, Zhaoab Y, Maa H, Yuan Z. Free vibration analysis of a rotating graphene nanoplatelet reinforced pre-twist blade-disk assembly with a setting angle. *Applied Mathematical Modelling*. 2021;93: 578-596.

[15] Eliseev V, Zinovieva T, Abid S. On the theory and methods of calculating the critical regimes of elastic rotor rotation. *Russian Internet Journal of Industrial Engineering*. 2017;5(3): 9-14.

[16] Polushkin O. Systematic laws of mechanics and balancing of rotors. *Bulletin of the Don State Technical University*. 2011;11(57): 842-849.

[17] Hui M, Qianbin Z, Xueyan Z, Qingkai H, Bangchun W. Dynamic characteristics analysis of a rotor–stator system under different rubbing forms. *Applied Mathematical Modelling, Elsevier*. 2015;39(8): 2392-2408.

[18] Solomin OV. Numerical methods for solving the equations of motion in problems of the dynamics of rotor systems with fluid friction supports. *Mechanical Engineering Magazine*. 2006;11: 16-26.

[19] Sperling L, Ryzhik B, Linz C, Duckstein H. Simulation of two-plane automatic balancing of a rigid rotor. *Mathematics and Computers in Simulation*. 2002;58: 351-365.

[20] Sašek JV. Eigenfrequency sensitivity analysis of flexible rotors. *Applied and Computational Mechanics*. 2007;1: 289-298.

[21] Kang Y, Chang Y, Tsai J, Mu L, Chang Y. An investigation in stiffness effects on dynamics of rotor-bearing-foundation systems. *Journal of Sound and Vibration*. 2000;231(2): 343-374.

[22] Mirsaidov M, Toshmatov E. Spatial stress state and dynamic characteristics of earth dams. *Magazine of Civil Engineering*. 2019;89(5): 3-15.

[23] Mirsaidov M, Troyanovsky I. Forced axisymmetric oscillations of a viscoelastic cylindrical shell. *Polymer Mechanics*. 1975;11(6): 953-955.

[24] Mirsaidov M, Mekhmonov Y. Nonaxisymmetric vibrations of axisymmetric structures with associated masses and hollows (protrusions). *Strength of Materials*. 1987;19(3): 424-430.

[25] Mirsaidov M, Abdikarimov R, Khudainazarov S, Sabirjanov T. Damping of high-rise structure vibrations with viscoelastic dynamic dampers. *E3S Web of Conferences*. 2020;224(02020): 1-14.
[26] Mirsaidov M, Dusmatov O, Khodjabekov M. The problem of mathematical modeling of a vibration protected rod under kinematic excitations. *IOP Conference Series: Materials Science and Engineering*. 2021;1030(1): 1-14.

THE AUTHORS

Ahmedov Olimjon
e-mail: olimjon84@mail.ru
ORCID: 0000-0002-1087-7303

Mirsaidov Mirziyod
e-mail: mirsaidov1948@mail.ru
ORCID: 0000-0002-8907-7869